Photonic Bandgap Fibres for Broadband Transmission of SWIR Wavelengths.

M.N. Petrovich[1], R. Amezcua-Correa[1], N.G. Broderick[1], D.J. Richardson[1],
T. Delmonte[2], M.A. Watson[2], E.J. O'Driscoll[2]
[1] Optoelectronics Research Centre, University of Southampton,
Southampton SO17 1BJ, UK
[2] BAE SYSTEMS Advanced Technology Centre,
Sowerby Building, FPC 267, PO Box 5, Filton, Bristol, BS34 7QW

Abstract

Hollow core photonic bandgap fibres can achieve light guidance in air, which offers a number of potential benefits for applications relevant to electro-magnetic remote sensing, including higher nonlinear and damage thresholds for high power beam delivery and operation at wavelengths that are not feasible using conventional fibres. Because they rely on coherent scattering from a highly ordered lattice of air holes as the mechanism of light guidance, bandgap fibres can only operate over a finite range of wavelengths. This paper investigates the parameters affecting the bandwidth of transmission in PBGFs and identifies realistic PBGF structures for wide-bandwidth operation in the SWIR wavelength region.

Keywords: Microstructured fibres, photonic bandgap fibres, infrared fibres

Introduction

Photonic bandgap fibres (PBGFs) are an emerging class of optical fibres that exploit photonic bandgap effects, rather than total internal reflection, as the mechanism of light guidance [1]. These fibres possess a periodic lattice of air holes acting as the cladding, in which light propagation is prohibited for well-defined ranges of optical frequencies. Optical modes are confined in a central core "defect", which can have lower refractive index than the cladding. Hollow core PBGFs are obtained by introducing an oversized air hole at the centre of the photonic crystal cladding. Such fibres allow for a very weak interaction of the guided mode with the fibre structure, which paves the way to novel and technologically enabling properties, such as low nonlinearity, high damage thresholds and transmission beyond silica's own transparency window [2].

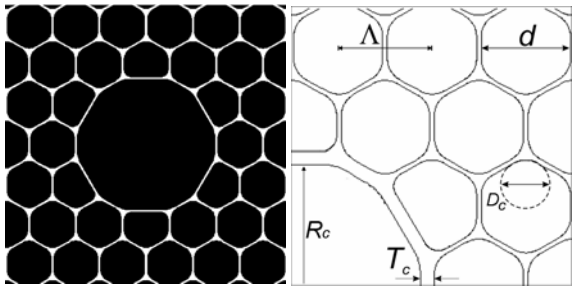

***Figure 1**. Cross section of a high-air filling factor PBGF and parameters used to define the structure.*

PBGFs are manufactured by the stack-and-draw method [2], much in the same way as index-guiding holey fibres. Fabrication of PBGFs is however more challenging because a very large air filling factor (>75%) and a small pitch are required for low loss operation [3]. Moreover, since light guidance in PBGFs relies upon resonant scattering from the photonic crystal lattice, the fibre transmission is strongly dependent on the structure and very sensitive to imperfections and to structural variations along the fibre length.

The position of the bandgap is primarily determined by the hole-to-hole spacing, Λ, and by the hole size and shape; since PBGFs require a high air filling factor, the holes are hexagonal with rounded corners and are generally described via two parameters (Fig 1): the relative hole diameter, d/Λ and the 'shape' factor, i.e. the relative radii of curvature at the corners, D_C/Λ [4].

The goal of this study is to develop PBGFs with broadband transmission in the short-wavelength infrared region (SWIR). To this end, two distinct factors must be considered. The first is the width of the optical bandgap, which is determined by the properties of the photonic crystal cladding. Secondly, the *operational bandwidth* of a PBGF must also take into account its wavelength dependent transmission loss. In particular, it is well established that PBGFs can support both core and surface modes [5] and coupling between these modes is a major source of loss in these fibres, and can drastically reduce the fibre's transmission bandwidth.

In this paper we present a detailed study of idealised but realistic PBGF structures, investigate the impact of key structural parameters and identify regimes that are robustly free of surface modes. Fibres fabricated with an optimised structure exhibit a wide low-loss operational bandwidth in good agreement with our theoretical predictions.

Transmission properties of PBGFs

Fig. 2 shows the optical bandgaps calculated for three different PBGF structures using a plane wave expansion method [6]. For a fixed wavelength λ_0, optical modes with effective index, $n^{eff}(\lambda_0)$, within the shaded areas cannot propagate in the photonic crystal cladding and are confined to the core. The fundamental air-guided mode has a dispersion curve (dashed line), which lies just below the "air line" (n^{eff}=1), thus the theoretical bandwidth of transmission ($\Delta\Lambda^{MAX}$) can be approximated by the intersection of the bandgap edges with the air line. Based on this definition, $\Delta\Lambda^{MAX}$ is only dependent on the properties of the cladding. Fig. 2 shows that increasing the hole size has a dramatic effect on the transmission bandwidth: as d/Λ is increased by less than 3% from 0.95 to 0.98, the bandgap almost doubles in width. This implies that a structure with very thin silica struts is preferable in order to achieve wide bandwidth PBGFs. The width of the bandgap is also found to depend on the shape factor, which also affects the air filling factor.

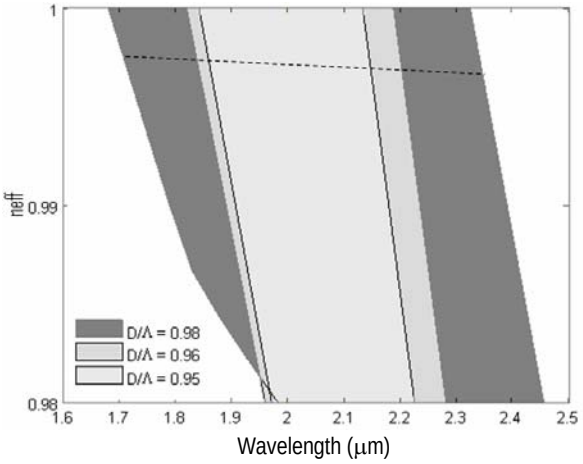

***Figure 2**: Optical bandgap of PBGF structures with d/Λ = 0.95, 0.96 and 0.98 for a fixed shape factor $D_C/\Lambda \approx 0.6$*

As stated above, the *operational bandwidth* of PBGFs depends on both the width of the optical bandgap and on the presence of surface modes (SMs). We employed a full vector finite element method (FEM) to accurately predict the dispersion curves of the optical modes supported by different PBGF structures. Fig. 3 shows a typical result for a fibre supporting one SM in addition to the 'fundamental' core mode. The top graph shows the dispersion curves (solid lines) superimposed on the optical bandgap (shaded region). The inserts show the mode profiles corresponding to the core mode (FM), with most of the optical power located in air, and of the SM, which is concentrated in the thin core boundary

region instead. An 'anticrossing' between modes occurs within the bandgap, which is indicated by a dashed square. The impact of such an 'interaction' between these modes can clearly be seen as a dip in the percentage of power in the core for the fundamental mode (bottom graph). Because surface modes are intrinsically lossy, an increase in the transmission loss of the FM is always observed at the anticrossing points [5]. The operational bandwidth is thus correspondingly reduced.

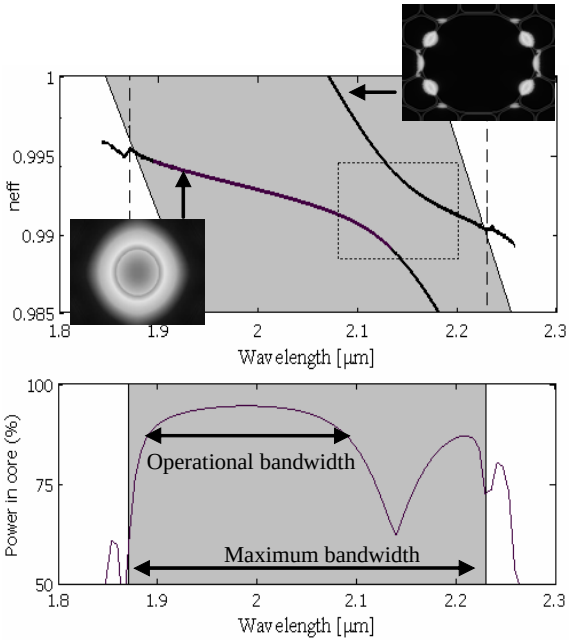

Figure 3*. (Top) Effective index of modes vs wavelength. (Bottom) Percentage of power in the core of the fundamental mode. Shaded regions represent the bandgap.*

To summarize, in order to achieve maximum bandwidth suitable PBGF structures must be identified where: a) the optical bandgap is widest and b) SMs are ideally eliminated, or at least their impact on the fibre transmission is minimised. This in turn involves two equally critical steps of optimizing both the cladding structure, which determines the width of the optical bandgap, and the design of the core boundary, which determines the presence of SMs and their position within the optical bandgap.

Optimisation of Fibre Design

In real PBGFs the core is defined by a thin non-circular silica ring of nearly constant thickness at the boundary with the cladding. During the fabrication at least two of the core parameters can be controlled, i.e. the thickness of the silica ring and the core diameter, while keeping the parameters of the cladding constant. Hence we have focused our study on the effects on the fibre's transmission properties due to the modification of these two parameters. The thickness of the core ring is described by the parameter T_C, while the size of the core is determined by its radii, R_C (Fig.1). Variations of R_C were modelled considering that only the first ring of holes is affected and the rest of the cladding is unchanged; this assumption was justified based on experimental observations, as clearly shown by two SEM micrographs of PBGFs with compressed and expanded cores (Fig. 4).

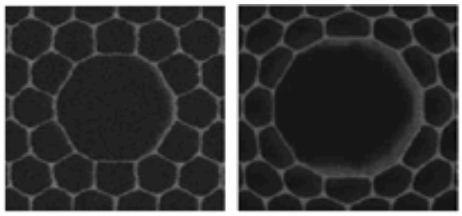

Figure 4. *SEM images of hollow-core PBGFs, with (a) compressed and (b) expanded core.*

We initially varied the core thickness T_C while holding the core size constant and calculated the optical modes within the bandgap. The analysis was then repeated for different values of R_C. Our detailed calculations showed a strong dependence of the number and position of SMs interacting with the core mode on T_C. It was however possible to identify a design regime, which is free of surface modes [7]. This 'optimum' core design regime requires the core ring to have a thickness of about half that of the struts within the photonic crystal cladding. Our calculations also showed that a further improvement in the operational bandwidth can be achieved in a design with a slightly compressed core [7]. By

performing a systematic study we established this to be a robust effect that does not critically depend on the core size or cladding properties. Furthermore, we have confirmed that the result holds true for both 7-cell core structures as well as for structures with a larger 19-cell core.

The modal and transmission properties of a PBGF with optimised structure are shown in Fig. 5, clearly demonstrating a huge improvement as compared to the un-optimized fibre structure in Fig. 2. Here SMs only occur either outside the optical bandgap or very close to its edges, hence they have very little impact on the fibre's transmission. Shaded areas indicate the width of the optical bandgap ($\Delta\Lambda^{MAX}$), which in this case approximately coincides with the operating bandwidth.

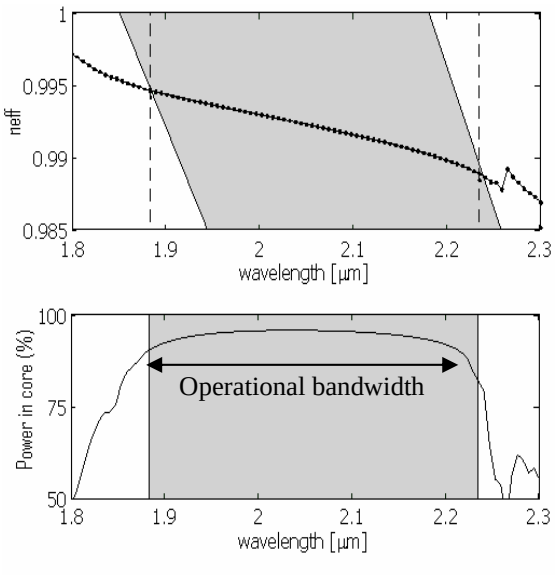

***Figure 5**. Modal dispersion curves of PBGFs with an 'optimised' structure.*

Fibre Fabrication

Fabrication of PBGFs with optimised structure was then undertaken. Several fibres were produced with bandgaps covering the range from 1.5 to 2.5μm. Detailed structural analysis was performed by scanning electron microscopy, which allowed us verification that the fibre's parameters were within the regime for wide bandwidth operation.

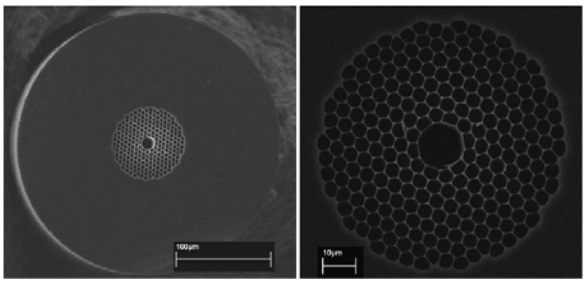

***Figure 6**. SEM images of fabricated PBGFs*

Fig. 6 shows a cross-sectional SEM image of a fibre with a 7-cell core and seven rings surrounding it, plus one incomplete ring to facilitate stacking and structure integrity during fibre fabrication. The fibre has a high air filling factor and the pitch of the photonic crystal cladding is in this case optimised for operation at about 2μm.

The fibre transmission was measured using an OPO source, which could be continuously tuned across the bandgap. Fig. 7 shows a plot of the total loss (fibre loss plus coupling loss) vs. wavelength. A 6m length was used in the measurements, which is deemed to be suitable for the end application of the present study. Little variation in the fibre transmission at the centre of the bandgap was however observed between samples with different fibre lengths, which indicates low fibre loss and good structural uniformity. Light transmitted at 2μm showed good beam quality ($M^2 \approx 1.4$).

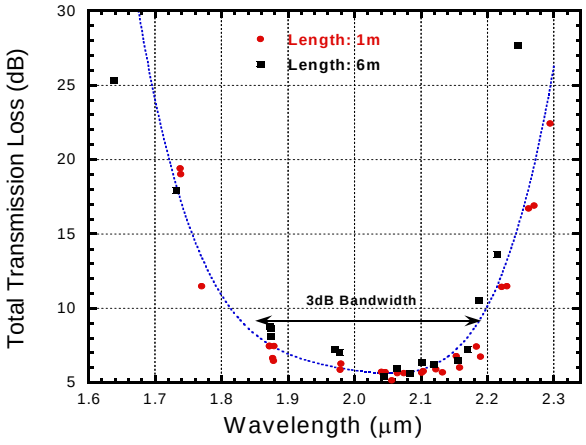

***Figure 7**. Bandwidth of transmission of a PBGF designed for operation at 2μm.*

All fibres produced showed a wide, low loss region completely free of surface modes; from the data shown in Fig.7, we estimated an operational bandwidth spanning approximately 350nm for the fibre operating at ≈2μm. This result is in very good agreement with the predictions of modelling shown in Fig. 5.

Conclusions

A detailed investigation of the factors affecting the bandwidth of transmission of PBGFs was presented. Through computer simulations we have shown that by carefully selecting the structural parameters it is possible to design PBGFs with high air filling fractions for which the fundamental mode is not affected by surface modes at all wavelengths within the bandgap, allowing maximum operational bandwidth. Several fibres with an optimized structure and operating wavelengths in the range 1.5 to 2.5μm were produced, demonstrating that the regimes identified through modeling are realistic and that the predicted operational bandwidths within these regimes closely match those experimentally measured in real fibres.

References

1 Cregan, R.F., Mangan, B.J., Knight, J.C., Birks, T.A., Russell, P.St.J., Roberts, P.J. and Allan, D.C., 1999, Science **285**, 1537-1539

2 Russell, P.St.J., Science **299**, 2003, 358-362

3 Brandon Shaw, L., Sanghera, J.S., Aggarwal, I.D. and Kung, F.H., 2003, Optics Express **11**(25), 3455-3460

4 Mortensen, N.A., Nielsen, M.D., Opt. Lett. 29(4), 349-350.

5 Smith, C.M., Venkataraman, N., Gallagher, M.T., Muller, D., West, J.A., Borrelli, NF, Allan, DC and Koch, KW, Nature 424 (2003) 657-659

6 Johnson, SG and Joannopoulos, JD, 2001 Optics Express **8**, (3), 173-190

7 Amezcua-Correa, R, Broderick, NGB, Petrovich, MN, Poletti, F, Richardson, DJ, Finazzi, V and Monro, TM, 2006, Proc OFC, paper OFC1

Acknowledgements

The work reported in this paper was funded by the Electro-Magnetic Remote Sensing (EMRS) Defence Technology Centre, established by the UK Ministry of Defence and run by a consortium of SELEX Sensors & Airborne Systems, Thales Defence, Roke Manor Research and Filtronic. R.A.C. thanks the Mexican Council for Science and Technology for support.